

Chapter 4

Betti Extended



In the previous chapter we repeatedly made use of the fact that the FE-solution $u_h(x)$ is the superposition of the **approximate influence function** $G_h(y, x)$ and the load $p(y)$

$$u_h(x) = \int_0^l G_h(y, x) p(y) dy. \tag{4.1}$$

This result is based on a theorem which we call *Betti extended*.

Theorem 4.1 (*Betti extended*) *One may replace the exact solutions u_1 and u_2 in Betti's theorem*

$$W_{1,2} = \int_0^l p_1 u_{2\uparrow} dx = \int_0^l p_2 u_{1\uparrow} dx = W_{2,1} \tag{4.2}$$

with the FE-approximations u_{1h} and u_{2h}

$$W_{1,2}^h = \int_0^l p_1 u_{2h\uparrow} dx = \int_0^l p_2 u_{1h\uparrow} dx = W_{2,1}^h. \tag{4.3}$$

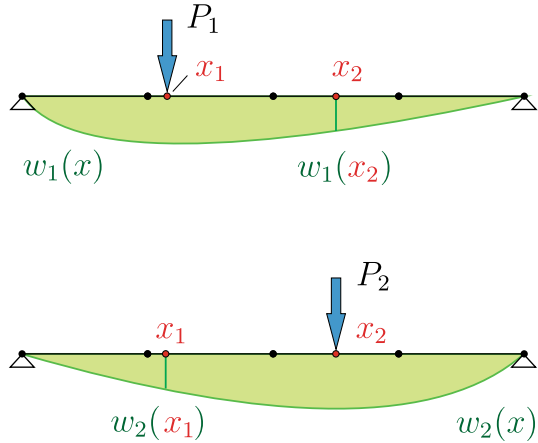
The claim is not that $W_{1,2}^h$ is the same as $W_{1,2}$, but rather: If $W_{1,2} = W_{2,1}$ is true, then $W_{1,2}^h = W_{2,1}^h$ is true as well; in short,

$$(p_1, u_2) = (p_2, u_1) \Rightarrow (p_1, u_{2h}) = (p_2, u_{1h}). \tag{4.4}$$

The best way to understand *Betti extended* is to focus on **Maxwell's theorem**, see Fig. 4.1, which is just a particular application of *Betti's theorem*

$$P_1 \cdot w_2(x_1) = P_2 \cdot w_1(x_2). \tag{4.5}$$

Fig. 4.1 *Maxwell's theorem*



If the two curves $w_1(x)$ and $w_2(x)$ are approximated with finite elements, the deflections at the two points x_1 and x_2 are not exact

$$w_{1h}(x_2) \neq w_1(x_2) \quad w_{2h}(x_1) \neq w_2(x_1), \tag{4.6}$$

but *Betti extended* guarantees that *Maxwell's theorem* holds true also in this situation

$$P_1 \cdot w_{2h}(x_1) = P_2 \cdot w_{1h}(x_2). \tag{4.7}$$

This feature extends *Maxwell's theorem* to FE-solutions, set $P_1 = P_2 = 1$, which is not necessarily self-evident. That it had to be true for the nodal values, is a consequence of the symmetry of the stiffness matrices. ***Betti extended*** guarantees this also for all points in between.

4.1 Proof

The proof of ***Betti extended*** is based on the two equations

$$\int_{\Omega} p_{1h} u_{2h} d\Omega = \int_{\Omega} p_1 u_{2h} d\Omega \tag{4.8a}$$

$$\int_{\Omega} p_{2h} u_{1h} d\Omega = \int_{\Omega} p_2 u_{1h} d\Omega, \tag{4.8b}$$

and ***Betti's theorem*** itself

$$\mathcal{B}(u_{1h}, u_{2h}) = \int_{\Omega} p_{1h} u_{2h} d\Omega - \int_{\Omega} p_{2h} u_{1h} d\Omega = 0. \tag{4.9}$$

This gives

$$\int_{\Omega} p_1 u_{2h} d\Omega = \int_{\Omega} p_{1h} u_{2h} d\Omega = \int_{\Omega} p_{2h} u_{1h} d\Omega = \int_{\Omega} p_2 u_{1h} d\Omega, \quad (4.10)$$

or

$$\int_{\Omega} p_1 u_{2h} d\Omega = \int_{\Omega} p_2 u_{1h} d\Omega, \quad (4.11)$$

which is *Betti extended*.

At Eq. (4.8a) we arrive as follows: According to the *Galerkin-orthogonality* we have

$$\delta W_i = a(u_1 - u_{1h}, \varphi_i) = 0, \quad (4.12)$$

or, if we write it as external instead of internal virtual work, $\delta W_i = \delta W_e$,

$$\int_{\Omega} (p_1 - p_{1h}) \varphi_i d\Omega = 0 \quad i = 1, 2, \dots, n \quad \Rightarrow \quad \int_{\Omega} (p_1 - p_{1h}) u_{2h} d\Omega = 0, \quad (4.13)$$

since u_{2h} is a linear combination of the φ_i . In the same way we arrive at the second equation.

With *Betti extended* the proof of the central Eq. (4.1) is easy, since in the influence function for $u(x)$

$$W_{1,2} = 1 \cdot u(x) = \int_0^l \delta(y-x) u(y) dy = \int_0^l G(y,x) p(y) dy = W_{2,1}, \quad (4.14)$$

we may replace u and G with the FE-solutions u_h and G_h

$$W_{1,2}^h = \int_0^l \delta(y-x) \underset{\uparrow}{u_h}(y) dy = \int_0^l \underset{\uparrow}{G_h}(y,x) p(y) dy = W_{2,1}^h, \quad (4.15)$$

and so

$$u_h(x) = \int_0^l G_h(y,x) p(y) dy. \quad (4.16)$$

This **switch**, $u \rightarrow u_h$ and $G \rightarrow G_h$, can be applied to all linear functionals

$$J(u) = \int_0^l \delta(y-y) u(y) dy = \int_0^l G(y,x) p(y) dy, \quad (4.17)$$

resulting in

$$J(u_h) = \int_0^l \delta(y - x) u_h(y) dy = \int_0^l G_h(y, x) p(y) dy. \quad (4.18)$$

4.2 At Which Points Is the FE-Solution Exact?

With the help of *Betti extended* we can now also specify when and where FE-results are exact.

We study this question with a prestressed rope. The influence function $G(y, x)$ for the deflection $u(x)$ of the rope, see Fig. 4.2, at the point $x = 1.5$ is the response of the rope to a single force $P = 1$, a **Dirac delta** $\delta(y - x)$.

Since the FE-program cannot generate this shape, it instead places two half as large single forces at the two neighboring nodes. This is—in our notation—the load case $\delta_h(y, x)$ and the corresponding deflection $G_h(y, x)$ is the approximate influence function.

So, there are **two Dirac deltas**, the exact and the approximate

$$\delta(y - x) \quad \downarrow \quad \delta_h(y - x) \quad \frac{1}{2} \downarrow + \frac{1}{2} \downarrow, \quad (4.19)$$

and also, **two influence functions**

$$G(y, x) \quad (\text{one peak}) \quad G_h(y, x) \quad (\text{two peaks}). \quad (4.20)$$

With finite elements we search for an approximate solution in the space \mathcal{V}_h , i.e. all the rope polygons, which can be generated with the three nodal shape functions $\varphi_i(x)$. Note, the dual of \mathcal{V}_h is the space \mathcal{V}_h^* of all load cases (nodal forces f_1, f_2, f_3), which create the rope polygons in \mathcal{V}_h .

Now, if a function u_h lies in \mathcal{V}_h (is a rope polygon), the approximate Dirac delta (2 half-sized single forces) is as good as the exact Dirac delta (one single force)

$$u_h(x) = \int_0^l \delta(y - x) u_h(y) dy = \int_0^l \delta_h(y - x) u_h(y) dy. \quad (4.21)$$

In concrete terms this means

$$1 \cdot u_h(x) = \frac{1}{2} \cdot u_h(x_1) + \frac{1}{2} \cdot u_h(x_2), \quad (4.22)$$

and this makes sense since the height of a straight line in between two nodes is just the average of the nodal values.

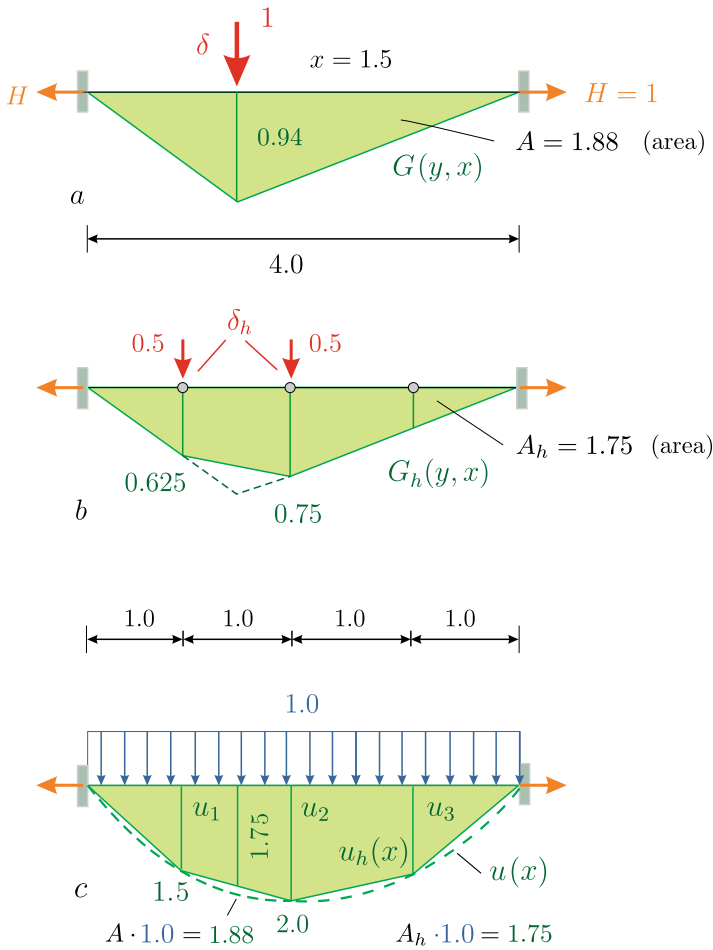


Fig. 4.2 Influence function for the deflection at the point $x = 1.5$, **a** exact influence function, **b** approximation, **c** FE-solution under uniform load $p = 1$

And because the **FE-load case** p_h lies in \mathcal{V}_h^* , i.e. consists of three nodal forces, the approximate influence function $G_h(y, x)$ is as good as the exact influence function

$$u_h(x) = \int_0^l G(y, x) p_h(y) dy = \int_0^l G_h(y, x) p_h(y) dy. \quad (4.23)$$

This too, is easy to understand. Since the load p_h consists of nodal forces f_i , the influence function is a sum over the nodes

$$u_h(x) = \int_0^l G_h(y, x) p_h(y) dy = \sum_{i=1}^3 G_h(y_i, x) f_i. \tag{4.24}$$

But each of the three nodal influence functions is exact, $G_h(y_i, x) = G(y_i, x)$, and this explains why the sum in (4.24) is $u_h(x)$ at each point x .

On \mathcal{V}_h and \mathcal{V}_h^* the results obtained with $\delta_h(y, x)$ and $G_h(y, x)$ respectively are exact.

And this is true for **any** function in \mathcal{V}_h , since (4.21) applies to all $u_h \in \mathcal{V}_h$. And since p_h lies in \mathcal{V}_h^* one can calculate any value $u_h(x)$ of the rope polygon with the approximate influence function $G_h(y, x)$. This is the essence of (4.24).

But that is not the end of it. The approximate Dirac delta, the two “half-sized” point loads at the neighboring nodes, constitute themselves a functional

$$J_h(u) = \int_0^l \delta_h(y - x) u(y) dy = \frac{1}{2} (u(x_1) + u(x_2)), \tag{4.25}$$

which can be applied to any function—not just the rope polygons in \mathcal{V}_h . Applied to $u(x) = \sin \pi x/4$ the result is

$$J_h(u) = \frac{1}{2} \left(\sin \frac{1.0\pi}{4} + \sin \frac{2.0\pi}{4} \right) = 0.85, \tag{4.26}$$

while $J(u) = \sin(1.5 \pi/4) = 0.92$. So, there is a difference between J and J_h .

However, regarding the exact solution $u(x)$ and its FE-approximation $u_h(x)$, the following ***h-permutation rule*** applies

$$\boxed{J_h(u) = J(u_h)} \tag{4.27}$$

which can easily be verified, since

$$J_h(u) = \frac{1}{2} (u(1.0) + u(2.0)) = \frac{1}{2} (1.5 + 2.0) = 1.75 \tag{4.28}$$

$$J(u_h) = u_h(1.5) = 1.75. \tag{4.29}$$

The functional $J_h(u)$ measures u at the two points $x = 1.0$ and $x = 2.0$, while the functional $J(u_h)$ measures u_h only at the source point $x = 1.5$. But both measurements produce the same result!

The *h-permutation rule* is based on the fact that an FE-solution can be written in six separate ways

$$\begin{aligned}
 u_h(x) &= \int_0^l G(y, x) p_h(y) dy = \int_0^l G_h(y, x) p(y) dy \\
 &= \int_0^l G_h(y, x) p_h(y) dy \\
 &= \int_0^l \delta(y, x) u_h(y) dy = \int_0^l \delta_h(y, x) u_h(y) dy \\
 &= \int_0^l \delta_h(y, x) u(y) dy, \tag{4.30}
 \end{aligned}$$

and if we also count the three formulas

$$u_h(x) = a(G, u_h) = a(G_h, u_h) = a(G_h, u), \tag{4.31}$$

which are **variants of Mohr’s integral**, then there are even nine.

The first two equations

$$J(u_h) = \int_0^l G(y, x) p_h(y) dy = \int_0^l G_h(y, x) p(y) dy = J_h(u) \tag{4.32}$$

formulate the *h-permutation rule*, which is of course applicable to any functional $J(u_h)$, not only the displacements $u(x)$.

Whether we superpose the exact influence function G with the FE-load p_h , or the approximate influence function G_h with the original load p , makes no difference—the result is the same.

Figure 4.3 illustrates this with a pier placed under a plate, which carries a heavy-duty truck. The exact influence for the pier reaction is plotted in Fig. 4.3a and the approximate function in Fig. 4.3b. The wheel loads of the truck represent the load p , and the block load is a graphical substitute for the FE-load p_h . We have only one formula for the exact pier reaction

$$R = \int_{\Omega} G(\mathbf{y}, \mathbf{x}) p(\mathbf{y}) d\Omega_{\mathbf{y}}, \tag{4.33}$$

but **three ways** to calculate the approximate pier reaction R_h

$$R_h = \int_{\Omega} G(\mathbf{y}, \mathbf{x}) p_h(\mathbf{y}) d\Omega_{\mathbf{y}} = \int_{\Omega} G_h(\mathbf{y}, \mathbf{x}) p_h(\mathbf{y}) d\Omega_{\mathbf{y}} = \int_{\Omega} G_h(\mathbf{y}, \mathbf{x}) p(\mathbf{y}) d\Omega_{\mathbf{y}}. \tag{4.34}$$

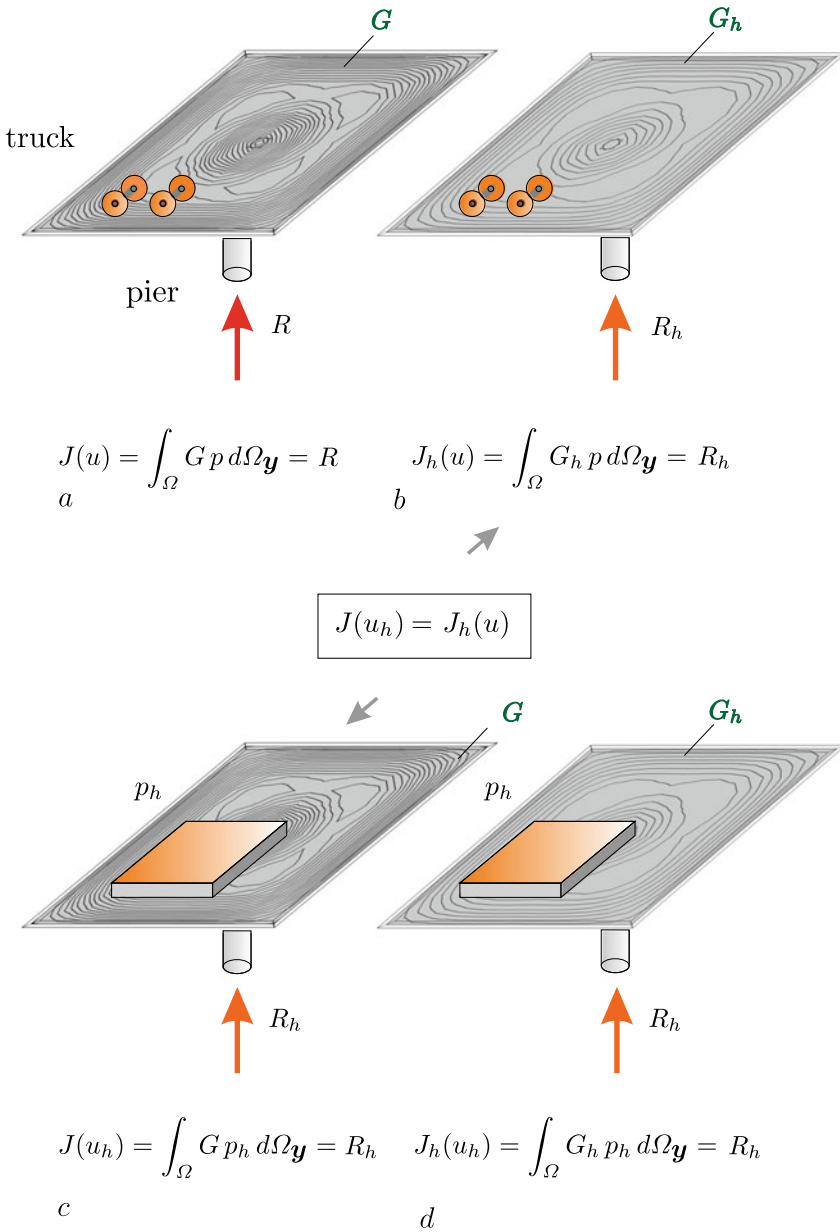


Fig. 4.3 Hinged plate with central pier. The four wheels of the truck, LC p , placed on the influence surface G_h gives the pier reaction R_h of the FE-solution. The same result is obtained, if the FE-load p_h (here pictured as a block load) is placed on the exact influence surface. And it is as well $R_h = (G_h, p) = (G_h, p_h)$, see Figure *b* and *d*

4.3 Exact Values

We can now also state, when the FE-solution is exact at a point.

Theorem 4.2 (*Exact values*)

Sufficient conditions

1. If the influence function G of a functional J lies in \mathcal{V}_h , its FE-approximation G_h is identical with G and therefore

$$J(u_h) = J_h(u) = J(u), \quad (4.35)$$

or

$$J(u_h) = (G, p_h) = (G_h, p) = (G, p) = J(u). \quad (4.36)$$

2. If the exact solution lies in \mathcal{V}_h , $u = u_h$, the error in any influence function is orthogonal to the right side p of the solution

$$J(u) - J(u_h) = \int_{\Omega} (G(\mathbf{y}, \mathbf{x}) - G_h(\mathbf{y}, \mathbf{x})) p(\mathbf{y}) d\Omega_{\mathbf{y}} = 0. \quad (4.37)$$

Necessary condition

1. If a value is exact, $J(u_h) = J(u)$, the error in the influence function must be orthogonal to the right side p

$$J(u) - J(u_h) = \int_{\Omega} (G(\mathbf{y}, \mathbf{x}) - G_h(\mathbf{y}, \mathbf{x})) p(\mathbf{y}) d\Omega_{\mathbf{y}} = 0. \quad (4.38)$$

4.4 One-Dimensional Problems

Since all influence functions are piecewise homogeneous solutions of the governing differential equation, exact nodal values, $u_h(x_i) = u(x_i)$, require the trial space \mathcal{V}_h to contain these solutions.

In 1-D problems such as $-EA u'' = p_x$ and $EI w^{IV} = p_z$ this is true, since the homogeneous solutions

$$u_h(x) = c_1 + c_2 x \quad (4.39a)$$

$$w_h(x) = c_1 + c_2 x + c_3 x^2 + c_4 x^3 \quad (4.39b)$$

lie in \mathcal{V}_h , see Fig. 4.2, but if a bar must work against some friction (c)